



## Radiation sensitive MOSFETs irradiated with various positive gate biases

Goran S. Ristic<sup>a</sup>, Stefan D. Ilic<sup>a</sup>, Russell Duane<sup>b</sup>, Marko S. Andjelkovic<sup>c</sup>, Alberto J. Palma<sup>d</sup>, Antonio M. Lallena<sup>d</sup>, Milos D. Krstic<sup>c</sup>, Srboljub J. Stankovic<sup>e</sup> and Aleksandar B. Jaksic<sup>b</sup>

<sup>a</sup>Faculty of Electronic Engineering, University of Niš, Niš, Serbia; <sup>b</sup>Tyndall National Institute, University College Cork, Cork, Ireland; <sup>c</sup>IHP, Leibniz-Institut Für Innovative Mikroelektronik, Frankfurt Oder, Germany; <sup>d</sup>Department of Electronics and Computer Technology, University of Granada, Granada, Spain; <sup>e</sup>Department of Radiation and Environmental Protection, "Vinča" Institute of Nuclear Sciences, Belgrade, Serbia

### ABSTRACT

The Radiation sensitive metal-oxide-semiconductor field-effect-transistors (RADFETs) were irradiated with gamma rays up to absorbed dose of 110 Gy(H<sub>2</sub>O). The results of threshold voltage,  $V_T$ , during irradiation with various positive gate biases showed the increase in  $V_T$  with gate bias. The threshold voltage shift,  $\Delta V_T$ , during irradiation was fitted very well. The contributions of both the fixed traps (FTs) and switching traps (STs) during radiation on  $\Delta V_T$  were analyzed. The results show the significantly higher contribution of FTs than STs. A function that describes the dependence of threshold voltage shift and its components on gate bias was proposed, which fitted the experimental values very well. The annealing at the room temperature without gate bias of irradiated RADFETs was investigated. The recovery of threshold voltage, known as fading, slightly increase with the gate bias applied during radiation. The  $\Delta V_T$  shows the same changes as the threshold voltage component due to fixed states,  $\Delta V_{ft}$ , while there is no change in the threshold voltage component due to switching traps,  $\Delta V_{st}$ .

### ARTICLE HISTORY

Received 18 January 2021  
Accepted 16 August 2021

### KEYWORDS

pMOS dosimeters; RADFETs; sensitivity; fading; radiation defects

## 1. Introduction

It has long been known that p-channel metal-oxide-semiconductor field-effect-transistors (pMOSFETs) with Al-gate can be used as dosimeters for ionizing radiation and hence their name pMOS dosimeters. They are currently used in radiation therapy (Rosenfeld et al., 2020), spacecraft (Hadi et al., 2019), and nuclear facilities (Mateu et al., 2018), but the application in personal dosimetry is still in the testing phase. The most common name for pMOSFETs used as radiation dosimeters (dosimetric pMOSFETs) is radiation sensitive field-effect transistors (RADFETs). New types of these transistors are being intensively investigated, with the use of new technologies (Abe et al., 2020; Cramer et al., 2018; Jain et al., 2020; Kahraman et al., 2020; Lai et al., 2017; Lee et al., 2018; Liu et al., 2016; Tamersit, 2019; Zeidell et al., 2020), as well as the commercial transistors (Carvajal et al., 2017). Very intensive researches are being carried out in order to improve the characteristics of RADFETs, primarily their sensitivity and recovery (Andreev et al., 2020; Aleksandrov, 2015; Biasi et al., 2020; Carbonetto et al., 2020; Dubey et al., 2018; Kulhar et al., 2019; Sampaio et al., 2020; Yilmaz et al., 2017).

This paper presents the results of RADFETs that are positively biased during irradiation by gamma-ray source and unbiased during annealing at room temperature. The idea is to examine how gate bias influences the changes in the threshold voltage shift and in

its components due to the creation of charge in the oxide and at the oxide/silicon interface. This is important for all types of applications of these dosimeters.

## 2. Experimental details

RADFETs manufactured at the Tyndall National Institute, Cork, Ireland were used in this study. They have 400-nm-thick oxide, and threshold voltage before radiation about 0.9 V (more details and pictures of used RADFETs can be found in (Andjelković et al., 2015; Ristic et al., 2015)).

The RADFETs were irradiated by gamma-radiation at room temperature using <sup>60</sup>Co ionizing source. The absorbed dose rate was  $D_R = 2.14 \cdot 10^{-3}$  Gy(H<sub>2</sub>O)/s and absorbed dose was  $D = 110$  Gy(H<sub>2</sub>O). The irradiation was performed in the Radiation and Environmental Protection Laboratory, Vinča Institute of Nuclear Science, Belgrade, Serbia.

During irradiation, the gate biases were  $V_G = 1, 3$  and 5 V. After the radiation, RADFETs were annealed at room temperature without gate bias ( $V_{Ga} = 0$  V).

A fully automatic system, containing a switching matrix and a source measure unit, was used for RADFET characterizations (see G.S. Ristić et al., 2011). The experiments were performed by a program written in the C# programming language. The main experimental set-up is given in (Andjelković et al., 2015; G.S. Ristić et al., 2011).

In order to quickly measure the electrical characteristics of the transistor, the gate and drain, as well as the source and bulk were short connected. The drain-source current was forced and the gate biases were measured. In this way, the measurement of the electrical characteristics of the transistor takes seconds.

A transistor threshold voltage,  $V_T$ , was determined as the intersection between  $V_G$  axis and the extrapolated linear region of the  $(I_D)^{1/2} - V_G$  curves, using the least square method performed by Octave 6.2.0 program (Ristić, 2008). The threshold voltage shift,  $\Delta V_T$ , is:

$$\Delta V_T = V_T - V_{T0} \quad (1)$$

where  $V_T$  is the transistor threshold voltage during both the radiation and room-temperature annealing, but  $V_{T0}$  is the transistor threshold voltage before radiation.

The midgap-subthreshold technique (MGT) (McWhorter & Winokur, 1986) that determines the contribution of fixed traps (FTs),  $\Delta V_{ft}$ , and contribution of switching traps (STs),  $\Delta V_{st}$ , to the threshold voltage shift,  $\Delta V_T$ , was used. Threshold voltage shift during radiation and annealing can be presented by these contributions:

$$\Delta V_T = \Delta V_{ft} + \Delta V_{st} \quad (2)$$

Using the  $\Delta V_{ft}$  and  $\Delta V_{st}$ , the areal density of FTs,  $\Delta N_{ft}$  [ $\text{cm}^{-2}$ ], and areal density of STs,  $\Delta N_{st}$  [ $\text{cm}^{-2}$ ], during radiation and annealing, for p-channel MOSFETs, can be calculated as:

$$\Delta N_{ft} = \frac{C_{ox}}{e} \Delta V_{ft}, \Delta N_{st} = \frac{C_{ox}}{e} \Delta V_{st} \quad (3)$$

where  $e$  is the absolute value of the electron charge and  $C_{ox}$  is the gate oxide capacitance per unit area.  $C_{ox} = \epsilon_{ox}/t_{ox}$ , where  $\epsilon_{ox} = 3.45 \times 10^{-13}$  F/cm is the silicon-dioxide permittivity, and  $t_{ox}$  is the oxide thickness.

The STs consist of traps near the oxide/substrate interface – slow switching traps (SSTs) and traps exactly at this interface – fast switching traps (FSTs) (Ristić, 2008). The  $\Delta N_{st}$  can be represented as:

$$\Delta N_{st} = \Delta N_{sst} + \Delta N_{fst} \quad (4)$$

where  $\Delta N_{sst}$  and  $\Delta N_{fst}$  are the areal densities of SSTs and FSTs, respectively.

### 3. Results and discussion

The changes in threshold voltage,  $V_T$ , during both the radiation with various positive gate biases ( $V_G = 1, 3$  and  $5$  V) and room-temperature annealing without gate bias ( $V_{G,a} = 0$  V), known as a spontaneous annealing, are presented in Figure 1. It can be seen that  $V_G$  influences the  $V_T$  in both cases, and that increase in  $V_T$  during radiation, and decrease in  $V_T$  during spontaneous annealing are bigger for higher  $V_G$ .

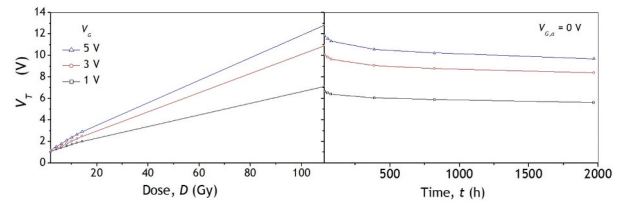


Figure 1. Threshold voltage during radiation and spontaneous annealing.

An equation that very well fitted the dependence of  $\Delta V_T$  on absorbed dose,  $D$ , was proposed in (G.S. Ristić et al., 2011; Ristic et al., 2015):

$$\Delta V_T(D) = \Delta V_{T,sat} - \frac{\Delta V_{T,sat}}{1 + b \cdot D^c} \quad (5)$$

where  $\Delta V_{T,sat}$ ,  $b$  and  $c$  are the positive constants. The  $\Delta V_{T,sat}$  represents the saturation value of  $\Delta V_T(D)$ .

We fitted the experimental results using Equation (5) and got a very good fit (Figure 2). The results showed very good agreement with Equation (5) and the  $r$ -square ( $r^2$ ) correlation coefficients were higher than 0.99 for all cases. Equation (5) fitted the  $\Delta V_T(D)$  much better than power law function:  $\Delta V_T(D) = b \cdot D^c$ , and exponential function:  $\Delta V_T(D) = b \cdot (1 - \exp(-c \cdot D))$ , where  $b$  and  $c$  are the positive constants. Yilmaz et al. (2017) and Kahraman et al. (2020) also used Equation (5) and obtained very well fit of  $\Delta V_T(D)$ .

Else, it is important to emphasize that Ristic et al. (2015) have shown that 5 or more points are enough to fit  $\Delta V_T = f(D)$  using Equation (5) very reliable. We performed a very detailed statistical analysis of the dependence of the reliability of the parameters  $\Delta V_{T,sat}$ ,  $b$  and  $c$  on the number of measured values during radiation. That analysis showed that a large number of points is not necessary during irradiation and that only a few of them, i.e. at least 5 points, at the beginning of irradiation, are sufficient to obtain a very reliable fit by Equation (5).

Figure 3 shows the threshold voltage shift,  $\Delta V_T$ , and its components induced by both the fixed traps (FTs),  $\Delta V_{ft}$ , and the switching traps (STs),  $\Delta V_{st}$ , during irradiation with gate bias  $V_G = 3$  V. As it can be seen, the influence of FTs is significantly higher than influence of STs on  $\Delta V_T$  (this is about 90%). The behavior for the

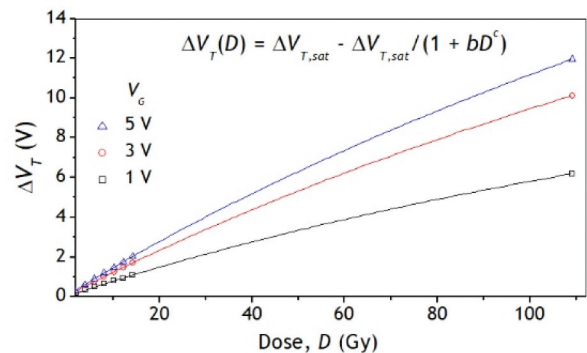
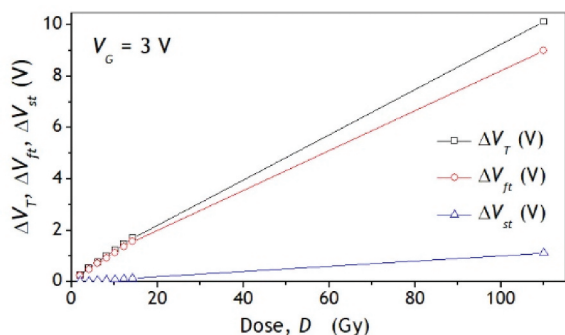


Figure 2. Fitting of threshold voltage shift,  $\Delta V_T$ , during radiation using Equation (5).



**Figure 3.**  $\Delta V_T$ ,  $\Delta V_{ft}$  and  $\Delta V_{st}$  during radiation.

other two gate biases is identical (not shown). An illustration of the electron excitation process during  $^{60}\text{Co}$  irradiation of MOSFETs is given in (Ristić, 2008).

During radiation, charged traps are formed in the oxide and at the interface. However, those charged oxide traps, which are close to the interface, have the same influence on the carriers in the channel as the interface traps themselves (Figure 4). When the electrical characteristics of transistors are used to classify defects, as in our case, then the influence of the charge on the carriers is crucial. That is why we have divided radiation defects into fixed traps (FTs), switching traps (STs), slow switching traps (SSTs) and fast switching traps (FSTs) (Ristić, 2008).

Increasing the positive voltage at the gate during irradiation leads to:

- (1) reducing the probability of recombination of electrons and holes at the place of their formation under the effect of radiation (electrons leave, holes are trapped),
- (2) increasing the probability that the trapped holes will move and reach the area near the interface where the energy deeper trapping centers are located.

These effects lead to increase in FTs and SSTs.

The FSTs are formed from hydrogen ions  $\text{H}^+$  that reach the interface. This means that an increase in positive gate bias also leads to an increase in these traps because it increases the probability that  $\text{H}^+$  ions reach interface.

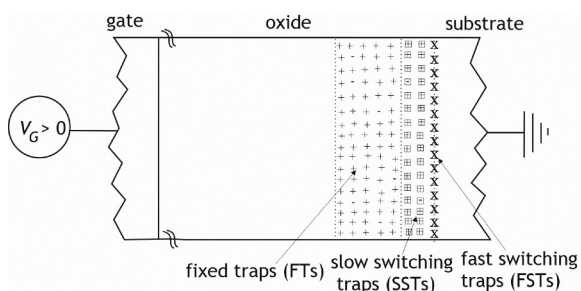


**Figure 4.** Distribution of traps induced by radiation.

**Table 1.** The parameters of Equation (6) fitted in Figure 5.  $\Delta V_{T,ft,st,sat}$ ,  $b$  and  $c$  are the positive constants.

@110 Gy	$\Delta V_{T,ft,st}$ (0 Gy)	$\Delta V_{T,ft,st,sat}$	$r$	$s$
$\Delta V_T$	2.710	13.55	0.80	0.68
$\Delta V_{ft}$	2.755	11.98	0.77	0.69
$\Delta V_{st}$	0.016	1.57	0.99	0.65

Our intention was to fit the dependencies of  $\Delta V_T$ ,  $\Delta V_{ft}$  and  $\Delta V_{st}$  on the gate bias  $V_G$ . We tried many functions, but the next function best fit the experimental results:

$$\Delta V_{T,ft,st}(V_G) = \Delta V_{T,ft,st,sat}(1 - r \cdot s^{V_G}) \quad (6)$$

where  $\Delta V_{T,sat}$  is the saturation value of  $\Delta V_T$ ,  $\Delta V_{ft,sat}$  is the saturation value of  $\Delta V_{ft}$ ,  $\Delta V_{st,sat}$  is the saturation value of  $\Delta V_{st}$ , but  $r$  and  $s$  are the positive constants.

The extrapolation of fitting curves to  $V_G = 0$  V shows that these values,  $\Delta V_{T,0 \text{ Gy}}$ ,  $\Delta V_{ft,0 \text{ Gy}}$ ,  $\Delta V_{st,0 \text{ Gy}}$ , are not equal zero, because there is an external positive electric field, even in this no gate bias case. Namely, for pMOSFETs with Al gate, like RADFETs used in this paper, for  $V_G = 0$  V (the zero-bias regime) a small positive gate bias of  $V_{wf} = 0.33$  V exists. It is due to a work function difference between the Al-gate and n-type silicon substrate, which resulted in a low external electric field in the gate oxide of  $E_{wf} \approx V_{wf}/t_{ox} = 0.825$  V/ $\mu\text{m}$ . This field has a direction toward the gate oxide/substrate ( $\text{SiO}_2/\text{Si}$ ) interface. The values of fitting parameters are given in Table 1.

The contribution of  $\Delta V_{ft}$  and  $\Delta V_{st}$  to  $\Delta V_T$  for dose of 110 Gy is shown in Figure 6. A slight increase in contribution of STs and a slight decrease in contribution of FTs can be observed. The explanation is that as the gate voltage increases, the traps in the oxide approach the interface, which means that part of the FTs is converted to the STs (see Figure 4).

Another important characteristic of RADFETs is the recovery of the threshold voltage during room temperature annealing without gate bias (spontaneous annealing). This is another dosimetric

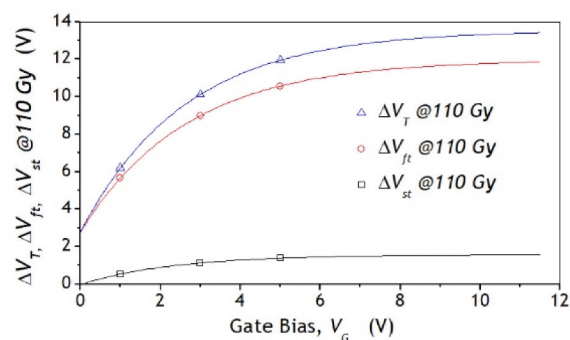


**Figure 5.**  $\Delta V_T$ ,  $\Delta V_{ft}$  and  $\Delta V_{st}$  at 110 Gy fitted by Equation (6).

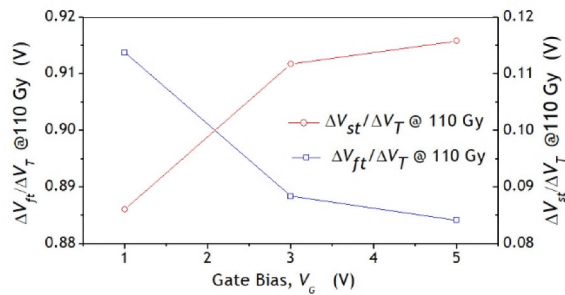


Figure 6.  $\Delta V_T$ ,  $\Delta V_{ft}$  and  $\Delta V_{st}$  at 110 Gy.

parameter, in addition to the sensitivity, of this dosimeter type, and is known as fading (G. Ristić et al., 1995; Ristić, 2009):

$$f = \frac{V_T(0) - V_T(t)}{V_T(0) - V_{T0}} = \frac{V_T(0) - V_T(t)}{\Delta V_T(0)} \quad (7)$$

where  $V_T(0)$  is the threshold voltage after radiation,  $V_T(t)$  is threshold voltage during room-temperature annealing, and  $V_{T0}$  is the transistor threshold voltage before radiation.

As can be seen in Figure 7, the fading significantly increases with the annealing time and slightly increases with the gate bias (after 2000 hours the fading is 24.01%, 25.08%, and 26.33%). This is a consequence of the increase in the tunneling of electrons from silicon to oxide, which leads to a decrease in the density of FTs and SSTs. However, small voltage differences lead to small changes in fading.

The behavior of threshold voltage shift and its components of RADFETs irradiated with  $V_G = 3 \text{ V}$  during spontaneous annealing is shown in Figure 8. The  $\Delta V_T$  has identical behavior as  $\Delta V_{ft}$ , but  $\Delta V_{st}$  is almost unchanged. The remaining two gate biases show the same behavior (not shown). It can be concluded that the annealing of fixed traps determines fading (Ristić et al, 2012).

#### 4. Conclusion

The obtained sensitivities at 110 Gy of the used transistors are 56.30 mV/Gy, 92.04 mV/Gy, and 108.69 mV/Gy for the gate bias of 1, 3, and 5 V. The threshold voltage increases with the gate bias, but this dependence is not linear. A function was proposed that describes the dependence

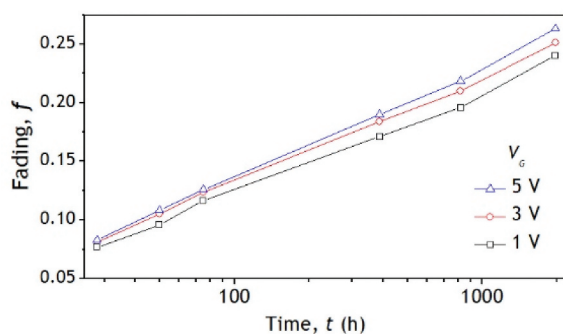


Figure 7. Fading of RADFETs biased with various voltages.

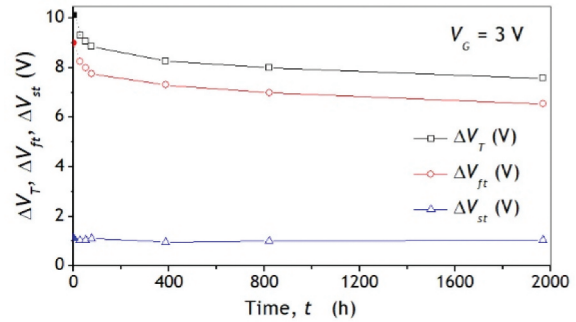


Figure 8.  $\Delta V_T$ ,  $\Delta V_{ft}$  and  $\Delta V_{st}$  during spontaneous annealing.

of the threshold voltage shift on the gate bias, and it fitted the obtained results very well. Based on this fitting, the saturation values of  $\Delta V_T$  is 13.55 V. The influence of fixed traps on the threshold voltage shift during radiation is about 90%. Fading is slightly increased by gate bias, and after 2000 hours the values are 24.01%, 25.08%, and 26.33%. The threshold voltage shift during spontaneous annealing is conditioned by the change in the density of fixed traps in the oxide.

#### Acknowledgments

The authors acknowledge the support by the European Union's Horizon 2020 research and innovation programme under grant agreement No. 857558, and the Ministry of Education, Science and Technological Development of the Republic of Serbia, under the project No. 43011.

#### Disclosure statement

No potential conflict of interest was reported by the author(s).

#### Funding

This work was supported in part by the European Union's Horizon 2020 research and innovation programme under grant agreement No. 857558, and the Ministry of Education, Science and Technological Development of the Republic of Serbia, under the project No. 43011.

#### ORCID

Goran S. Ristic <http://orcid.org/0000-0001-7603-6243>  
 Stefan D. Ilic <http://orcid.org/0000-0002-1721-9039>  
 Russell Duane <http://orcid.org/0000-0003-3702-1035>  
 Alberto J. Palma <http://orcid.org/0000-0001-9050-5413>  
 Antonio M. Lallena <http://orcid.org/0000-0003-1962-6217>  
 Aleksandar B. Jaksic <http://orcid.org/0000-0002-4668-6381>

#### References

Abe, Y., Umeda, T., Okamoto, M., Harada, S., Yamazaki, Y., & Ohshima, T. (2020). The effect of  $\gamma$ -ray irradiation on optical properties of single photon sources in 4H-SiC MOSFET. *Materials Science Forum*, 1004, 361–366. <https://doi.org/10.4028/www.scientific.net/msf.1004.361>

- Aleksandrov, O. V. (2015). On the effect of bias on the behavior of MOS structures subjected to ionizing radiation. *Semiconductors*, 49(6), 774–779. <https://doi.org/10.1134/S1063782615060020>
- Andjelković, M. S., Ristić, G. S., & Jakšić, A. B. (2015). Using RADFET for the real-time measurement of gamma radiation dose rate. *Measurement Science & Technology*, 26(2), 025004-1-12. <https://doi.org/10.1088/0957-0233/26/2/025004>
- Andreev, D. V., Bondarenko, G. G., Andreev, V. V., & Stolyarov, A. A. (2020). Use of high-field electron injection into dielectrics to enhance functional capabilities of radiation MOS sensors. *Sensors*, 20(8), 2382–1-11. <https://doi.org/10.3390/s20082382>
- Biasi, G., Su, F.-Y., Al Sudani, T., Corde, S., Petasecca, M., Lerch, M. L. F., Perevertaylo, V. L., Jackson, M., & Rosenfeld, A. B. (2020). On the combined effect of silicon oxide thickness and boron implantation under the gate in MOSFET dosimeters. *IEEE Transactions on Nuclear Science*, 67(3), 534–540. <https://doi.org/10.1109/TNS.2020.2971977>
- Carbonetto, S., Echarri, M., Lipovetzky, J., Garcia-Inza, M., & Faigón, A. (2020). Temperature-compensated MOS dosimeter fully integrated in a high-voltage 0.35  $\mu\text{m}$  CMOS process. *IEEE Transactions on Nuclear Science*, 67(6), 1118–1124. <https://doi.org/10.1109/TNS.2020.2966567>
- Carvajal, M. A., Escobedo, P., Jiménez-Melguizo, M., Martínez-García, M. S., Martínez-Martí, F., Martínez-Olmos, A., & Palma, A. J. (2017). A compact dosimetric system for MOSFETs based on passive NFC tag and smartphone. *Sensors and Actuators A: Physical*, 267, 82–89. <https://doi.org/10.1016/j.sna.2017.10.015>
- Cramer, T., Fratelli, I., Barquinha, P., Santa, A., Fernandes, C., D'Annunzio, F., Lousset, C., Martins, R., Fortunato, E., & Fraboni, B. (2018). Passive radiofrequency x-ray dosimeter tag based on flexible radiation-sensitive oxide field-effect transistor. *Science Advances*, 4(6), eaat1825-1-7. <https://doi.org/10.1126/sciadv.aat1825>
- Dubey, A., Singh, A., Narang, R., Saxena, M., & Gupta, M. (2018). Modeling and simulation of junctionless double gate radiation sensitive FET (RADFET) dosimeter. *IEEE Transactions on Nanotechnology*, 17(1), 49–55. <https://doi.org/10.1109/TNANO.2017.2719286>
- Hadi, S. A., Humood, K. M., Jaoude, M. A., Abunahla, H., Al Shehhi, H. F., & Mohammad, B. (2019). Bipolar Cu/HfO<sub>2</sub>/p<sup>++</sup> Si memristors by sol-gel spin coating method and their application to environmental sensing. *Scientific Reports*, 9, 9983–1-15. <https://doi.org/10.1038/s41598-019-46443-x>
- Jain, S., Gajarushi, A. S., Gupta, A., & Rao, V. R. (2020). A passive gamma radiation dosimeter using graphene field effect transistor. *IEEE Sensors Journal*, 20(6), 2938–2944. <https://doi.org/10.1109/JSEN.2019.2958143>
- Kahraman, A., Deevi, S. C., & Yilmaz, E. (2020). Influence of frequency and gamma irradiation on the electrical characteristics of Er<sub>2</sub>O<sub>3</sub>, Gd<sub>2</sub>O<sub>3</sub>, Yb<sub>2</sub>O<sub>3</sub>, and H<sub>2</sub>O<sub>2</sub> MOS-based devices. *Journal of Materials Science*, 55, 7999–8040. <https://doi.org/10.1007/s10853-020-04531-8>
- Kulhar, M., Dhoot, K., & Pandya, A. (2019). Gamma dose rate measurement using RadFET. *IEEE Transactions on Nuclear Science*, 66(10), 2220–2228. <https://doi.org/10.1109/TNS.2019.2942955>
- Lai, S., Cosseddu, P., Basiricò, L., Ciavatti, A., Fraboni, B., & Bonfiglio, A. (2017). A highly sensitive, direct X-ray detector based on a low-voltage organic field-effect transistor. *Advanced Electronic Materials*, 3, 1600409–1-7. <https://doi.org/10.1002/aeml.201600409>
- Lee, K. K., Wang, D., Shinobu, O., & Ohshima, T. (2018). Reliability of gamma-irradiated n-channel ZnO thin-film transistors: Electronic and interface properties. *Radiation Effects and Defects in Solids*, 173(5–6), 250–260. <https://doi.org/10.1080/10420150.2018.1427093>
- Liu, H., Yang, Y., & Zhang, J. (2016). A metal-oxide-semiconductor radiation dosimeter with a thick and defect-rich oxide layer. *Journal of Micromechanics and Microengineering*, 26(4), 045014–1-7. <https://doi.org/10.1088/0960-1317/26/4/045014>
- Mateu, I., Glaser, M., Gorine, G., Moll, M., Pezzullo, G., & Ravotti, F. (2018). ReadMON: A portable readout system for the CERN PH-RADMON sensors. *IEEE Transactions on Nuclear Science*, 65(8), 1700–1707. <https://doi.org/10.1109/TNS.2017.2784684>
- McWhorter, P. J., & Winokur, P. S. (1986). Simple technique for separating the effects of interface traps and trapped-oxide charge in metal-oxide-semiconductor transistors. *Applied Physics Letters*, 48(2), 133–135. <https://doi.org/10.1063/1.96974>
- Ristić, G., Golubović, S., & Pejović, M. (1995). P-channel metal-oxide-semiconductor dosimeter fading dependencies on gate bias and oxide thickness. *Applied Physics Letters*, 66(1), 88–89. <https://doi.org/10.1063/1.114155>
- Ristić, G. S. (2008). Influence of ionizing radiation and hot carrier injection on metal-oxide-semiconductor transistors. *Journal of Physics D: Applied Physics, Topical Review*, 41(2), 023001-1-19. <https://doi.org/10.1088/0022-3727/41/2/023001>
- Ristić, G. S. (2009). Thermal and UV annealing of irradiated pMOS dosimetric transistors. *Journal of Physics D: Applied Physics*, 42(13), 135101-1-12. <https://doi.org/10.1088/0022-3727/42/13/135101>
- Ristić, G. S., Vasović, N. D., & Jakšić, A. B. (2012). The fixed oxide traps modelling during isothermal and isochronal annealing of irradiated RADFETs. *Journal of Physics D: Applied Physics*, 45, 305101-1-11. <https://doi.org/10.1088/0022-3727/45/30/305101>
- Ristić, G. S., Vasović, N. D., Kovačević, M., & Jakšić, A. B. (2011). The sensitivity of 100 nm RADFETs with zero gate bias up to dose of 230 Gy(Si). *Nuclear Instruments and Methods in Physics Research Section B*, 269(23), 2703–2708. <https://doi.org/10.1016/j.nimb.2011.08.015>
- Ristic, G. S., Andjelkovic, M. S., & Jaksic, A. B. (2015). The behavior of fixed and switching oxide traps of RADFETs during irradiation up to high absorbed doses. *Applied Radiation and Isotopes*, 102, 29–34. <https://doi.org/10.1016/j.apradiso.2015.04.009>
- Rosenfeld, A. B., Biasi, G., Petasecca, M., Lerch, M. L. F., Villani, G., & Feygelman, V. (2020). Semiconductor dosimetry in modern external-beam radiation therapy. *Physics in Medicine & Biology*, 65(16), TR01. <https://doi.org/10.1088/1361-6560/aba163>
- Sampaio, J. M., Goncalves, P., Pinto, M., Silva, J., Negirneac, V., Sintra, L., Pinto, C., Sousa, T., Ribeiro, P., & Poivey, C. (2020). Dose measurements and simulations of the RADFETs response onboard the Alphasat CTTB experiments. *IEEE Transactions on Nuclear Science*, 67(9), 2028–2033. <https://doi.org/10.1109/TNS.2020.3013035>
- Tamersit, K. (2019). Performance assessment of a new radiation dosimeter based on carbon nanotube field-effect transistor: A quantum simulation study. *IEEE Sensors Journal*, 19(9), 3314–3321. <https://doi.org/10.1109/JSEN.2019.2894440>
- Yilmaz, E., Kahraman, A., McGarrigle, A. M., Vasovic, N., Yegen, D., & Jaksic, A. (2017). Investigation of RadFET response to X-ray and electron beams. *Applied Radiation and Isotopes*, 127, 156–160. <https://doi.org/10.1016/j.apradiso.2017.06.004>
- Zeidell, A. M., Ren, T., Filston, D. S., Iqbal, H. F., Holland, E., Bourland, J. D., Anthony, J. E., & Jurchescu, O. D. (2020). Organic field-effect transistors as flexible, tissue-equivalent radiation dosimeters in medical applications. *Advanced Science*, 7(18), 2001522–1-9. <https://doi.org/10.1002/adv.202001522>